DE GRUYTER OPEN

Journal of ELECTRICAL ENGINEERING, VOL 68 (2017), NO5, 371–377

The artificial neural network modelling of the piezoelectric actuator vibrations using laser displacement sensor

Levent Paralı[*], Ali Sarı[**], Ulaş Kılıç[***], Özge Şahin[****], Jiří Pěchoušek[*****]

We report an improvement of the artificial neural network (ANN) modelling of a piezoelectric actuator vibration based on the experimental data. The controlled vibrations of an actuator were obtained by utilizing the swept-sine signal excitation. The peak value in the displacement signal response was measured by a laser displacement sensor. The piezoelectric actuator was modelled in both linear and nonlinear operating range. A consistency from 90.3 up to 98.9% of ANN modelled output values and experimental ones was reached. The obtained results clearly demonstrate exact linear relationship between the ANN model and experimental values.

K e y w o r d s: piezoelectric actuator, laser displacement sensor, resonance frequency, vibration displacement, artificial neural network

1 Introduction

Piezoelectric materials are widely used as smart structures due to their inherent transducer characteristics. Functioning as actuators, they convert electrical energy into mechanical and contrary, transform mechanical energy into electrical when operating as sensors [1]. Piezoelectric actuators (PEAs) find a wide application in atomic force microscopes [2], accelerator based imaging systems [3], machine tools [4], computer components [5], industrial and medical robots [6] mainly due to their effective displacement capabilities. PEA's mechanical displacement characterization is a core issue in scientific and industrial research [7, 8].

The mechanical displacement of a vibrating surface is determined as a change of distance from the reference/zero position (equilibrium condition). A vibration of PEA can be described by the displacement, velocity, and acceleration, separately or together, in the given excitation frequency ranges [9, 10]. The dynamic testing of PEAs relates mainly sweep-sine excitations with displacement measurements. Computer-based measurement techniques are widely employed to control PEA vibration due to their high sensitivity and precision [11, 12].

A PEA represent a coupled electro-mechanical-acoustic system with frequency dependent properties characterized by device dimensions and used material. The analysis and design of the PEA are commonly performed by using lumped element models (LEM). Prasad and Gallas *et al* defined the velocity of the clamped piezoelectric-driven device (excited alternative voltage) via a scanning laser vibrometer and integrating the velocity in the frequency domain to obtain displacement under various conditions. They carried out both the electro–acoustic model and the LEM of a piezoelectric-driven device (constituted of a thin piezo–ceramic disk glued on a metallic shim). These model approaches are validated against experimental measurements, [13-15]. Especially, Chiatto *et al* presented a comprehensive review covering the development and the evolution of LEM of predicting the frequency response of piezo-driven synthetic jet devices, commonly used to control fluid flows [16].

In many vibration applications, the structure of the vibration is defined by mathematical models. Many studies have reported the linear operation of PEAs, [17-20]. Nevertheless, if PEA is exposed to a changing excitation voltage, the nonlinear operating conditions could occur due to its limited capacity. Under the nonlinear working conditions, some adverse effects associated with nonlinear dynamics, hysteresis, and saturation could cause problems, such as a loss of performance and a resonance frequency shift. Therefore, the nonlinear control techniques such as: (i) the Preisach model, (ii) a nonlinear autoregressive moving average model with exogenous inputs (NARMAX), and (iii) Artificial Neural Network (ANN) modelling has been improved to solve the nonlinear problems. Especially, neural networks are widely used because of their high precision approximation capabilities and a strong ability to be fault tolerant in the identification process [21, 22]. For instance, Ahn *et al* [23] used the neural networks on hybrid-type active vibration isolation, Liu

* Department of Electronics and Automation, levent.parali@cbu.edu.tr, ** Department of Electric and Energy, 45400 Turgutlu, Manisa, Turkey, *** Ege University, Faculty of Engineering, Department of Electrical & Electronics Engineering 35100 Bornova, Izmir, Turkey, **** Dokuz Eylul University, Faculty of Engineering, Department of Electrical & Electronics Engineering 35160 Buca, Izmir, Turkey ***** Department of Experimental Physics, Faculty of Science, Palack University in Olomouc, 17. listopadu 1192/12, 771 46 Olomouc, Czech Republic

DOI: 10.1515/jee-2017–0069, Print (till 2015) ISSN 1335-3632, On-line ISSN 1339-309X

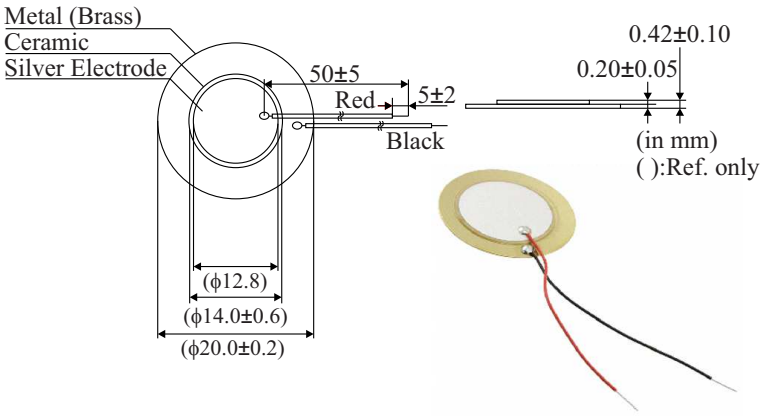

Fig. 1. Schematically displayed the tested PEA(7BB-20-6) with real dimensions. PZT layer is adhered onto a brass plate

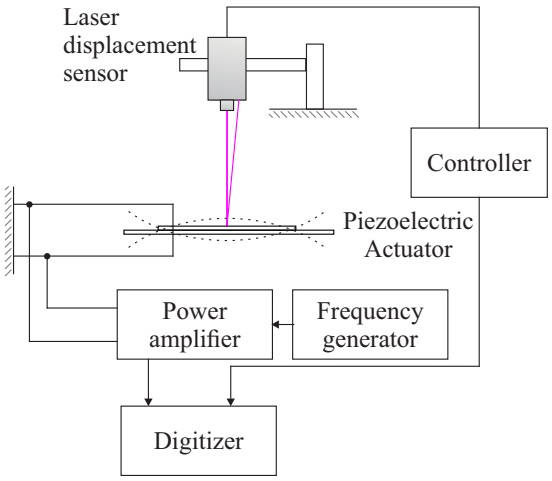

Fig. 2. Experimental setup of the digital measurement system based on LDS (Keyence) and measurement boards (National Instruments) controlled by LabVIEW application, [26]

and Zhang [24] reported the fault detection and diagnosis based on parameter estimation and neural network, Chen [25] used neural networks for structural fault diagnosis.

Modern nonlinear modelling methods are successfully used to describe nonlinear systems. One of these methods is ANN, based on many calculations performed by parallel operation of nonlinear elements. Due to the parallel learning process, fast response and adaptation features, ANN is probably one of the best information processing systems.

As it is well known, ANN can described as

$$Y = f(\sum_{i=1}^{m} w_i\, x_i) \qquad (1)$$

where, the input $x_1, \ldots, x_m$ is transferred through processing elements via internal connections. Each connection has a weight $w_1, \ldots, w_m$ which impacts particular element [25]. This can be positive, null, and negative. The transfer function behaves as a sum of the processing elements outputs which use all inputs in the calculation. The activation function arrange predetermined output of unlimited input processing elements. The four the most used activation functions are: linear, threshold, step, and sigmoid.

2 Material and methods

In this study, we used PEA sound component of Murata Manufacturing Co., Ltd. [24] with known parameters (see Table 1) namely 7BB-20-6. The diaphragm structure of PEA is made by adhering of the Lead Zirconate Titanate (PZT) onto a brass plate. The drawing of PEA is shown in Fig. 1.

Table 1. Specific parameters of PEA tested in this study

Plate size diameter, D (mm)	20
Element size diameter, a (mm)	14
Electrode size diameter, b (mm)	12.8
Thickness, T (mm)	0.42
Metal plate thickness, t_m (mm)	0.2
Resonance frequency, f_r (kHz)	6.3 ± 0.6
Capacitance, C (nF)	10± 30%
Dielectric Constant, ε_r	1510
Resonant Impedance, R (Ω)	≤ 300
Input voltage, V_{p-p} max (V)	30
Operating temperature, t_C °C	-20∼ 70

Table 2. Measurement capabilities of the LK-G37 (LDS) used in the experimental part

Measuring range	30± 5 mm
Adjustment time	0.06 ms
Repeatability	0.05 μm
Spot shape	Φ30 mm
Sampling rate	20 μs
Accuracy	± 0.02%

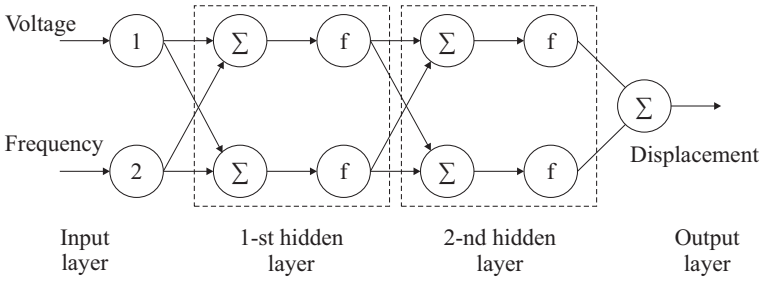

Fig. 3. The final structure of ANN model, used in this study for modelling PEA vibration

The vibration properties of the studied PEA were experimentally measured at room temperature employing the LK-G37 laser displacement sensor (LDS), and controlled by the LK-G3001 controller (Keyence) [25]. Measurement parameters of LDS are listed in Table 2.

2.1 Experimental Setup

The concept of the vibrometry system uses virtual instrumentation technique utilized in LabVIEW^{TM} (National Instruments). Figure 2 shows an experimental setup of the system.

The control and data read-out system consists of a personal computer with two PCI measurement boards. As a drive signal generator (excitation voltage) for PEA vibration control NI PCI-6115 board was used. An analog signal obtained from the LDS was processed on an analog input channel of the digitizer, NI PCI-5122. Setting of LDS device was performed separately through the Navigator program (Keyence). Before the initiating of the measurement application, the precise arrangement had to be set. The detailed configuration of the measurement system is presented in [26]. The laser beam was focused to the center of PEA disc. Analytically, boundary conditions of the PEA can be specified as completely free or any forced situations. The completely free boundary means that the PEA is floating in space with no attachment or connection in the ground and exhibits rigid body behavior at zero frequency. However, in the experimental works, it is not possible to fully obtain free condition. Therefore, to model the completely free boundary, the PEA must be supported by using some methods during test [27].

Mentioned measurement system is capable to measure the dynamic displacement as PEA vibration response using the swept-sine excitation method [26]; from *ie* 10 Hz up to 40 kHz with 1 Hz step.

4 ANN modelling of PEA vibration

The ANN modeling of PEA vibration behavior uses real experimental data obtained previously in [26]. After finding the minimum and maximum displacement values at the given voltage and frequency, the values were normalized. The data preparation process is described further.

4.1 Model structure

The proposed ANN model for the nonlinear behavior of PEA has two inputs: voltage and frequency. The displacement is used as an output. In this study, we used a multi-layer feed-forward back propagation neural network with Levenberg-Marquardt algorithm, which minimizes the sum of the mean squared error. The Levenberg-Marquardt algorithm derived from the steepest descent and Newton algorithms, is given by the equation

$$\Delta w = (\boldsymbol{J}^{\top}\boldsymbol{J} + \mu \boldsymbol{I})^{-1}\boldsymbol{J}^{\top}e, \tag{2}$$

where w is a weight vector, $\boldsymbol{J}$ is the Jacobian matrix, μ is combination coefficient, $\boldsymbol{I}$ is an identity matrix, e is an error vector, and μ is an adjustable parameter. Overlarging μ parameter leads to the algorithm behavior as the steepest descent method. Otherwise, it behaves as the Newton's method. Update algorithm for μ is given by

$$\mu(n) = \begin{cases} \mu(n-1)k & \text{for} E(n) > E(n-1) \\ \mu(n-1)/k & \text{for} E(n) \leq E(n-1) \end{cases} \tag{3}$$

ANN model consists of the thirty fully connected hidden layers set. The so-called *logistic* activation function was used for each input layer and for ANN output layer

$$f(n) = \frac{1}{1+\exp^{-n}} \tag{4}$$

The proposed ANN model was designed by the following steps:

- Minimum and maximum displacement values were found for each excitation voltage value.
- Each displacement value was normalized, to be 0-1.
- Data set was divided into training and test sets.
- After being educated by the training set, the model was examined via the testing set.
- The results of testing obtained from the ANN were converted to actual values.
- Error calculations were performed by different statistical methods such as mean square error and mean absolute error.

Figure 3 shows the final structure of ANN model.

4.2 Preparation of the experimental data

The changes in displacement of PEA surface were measured for frequencies between 5001 and 8000 kHz with the step of 1 Hz and recorded for amplitudes of excitation voltages from 0.5 to 10 V with the step of 0.5 V. Thus,

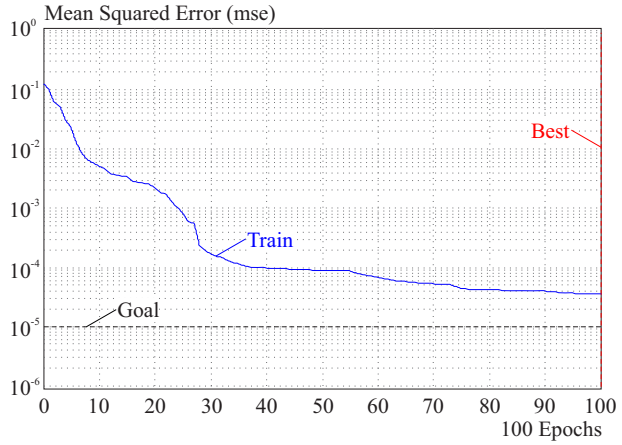

Fig. 4. ANN performance, shown as MSE value dependency on the epoch number

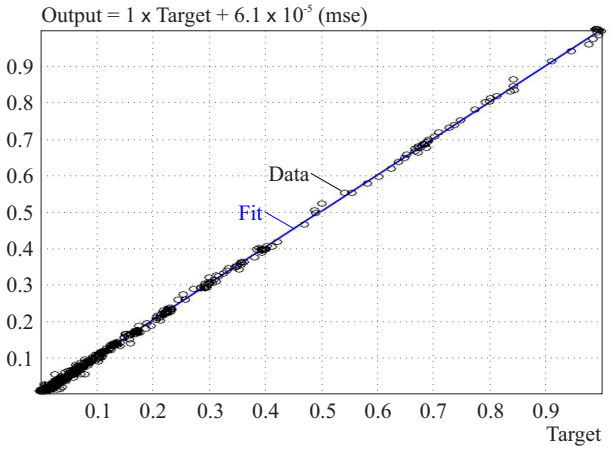

Fig. 5. Regression curve displayed for Case 6, when the training set includes 600 data and testing set includes 59400 data.

the displacements were measured for 60000 different input values. Minimum and maximum displacement values were normalized by [28, 29]

$$\begin{aligned} Y_j^{min} &= \min(y_{i,j}) \\ Y_j^{max} &= \max(y_{i,j}) \\ i &= 5001, \ldots, 8000 \\ j &= 0.5, 1.0, \ldots, 10 \\ Y_i^{norm} &= \frac{y_i - y_j^{min}}{y_j^{max} - y_j^{min}} \\ i &= 1, \ldots, 60000 \\ j &= 0.5, 1.0, \ldots, 10 \end{aligned} \tag{5}$$

Table 3 shows the data set.

Table 3. Preparation for data processing

Frequency(Hz)	Voltage (V)				
	0.5	1	...	9.5	10
5001	y_2	y_3001	...	$y_5$4001	$y_5$7001
5002	...	y_3002	...	$y_5$4002	$y_5$7002
...	...	...	...	...	...
8000	$y_2$999	$y_5$999	...	$y_5$6999	$y_6$0000

The normalized values used for training and testing of ANN were converted to the real values by

$$\begin{aligned} Y_i^{ANN} &= y_i^{norm}(y_j^{max} - y_j^{min}) + y_j^{min} \\ i &= 1, \ldots, 60000 \\ j &= 0.5, 1.0, \ldots, 10 \end{aligned} \tag{6}$$

4.3 Modelling results

For designing the proposed ANN model the Neural Network Toolbox (Matlab) was used. The data set includes 60000 points and the whole data set consists of two groups: training and testing sets. The data were examined for six different situations are shown in Table 4.

Table 4. Distrubution of examined six different situations

Situation	Number of data in set:	
	Training	Testing
Case		
1	30000	30000
2	20000	40000
3	15000	45000
4	12000	48000
5	6000	54000
6	600	59400

The proposed algorithms were carried out 20 times for each case. Determination coefficient (R^2), mean square error (MSE) and mean absolute error (MAE) were calculated for each situation

$$\begin{aligned} R^2 &= \frac{F_0 - F}{F_0}, \\ F_0 &= \sum_{i=1}^{n} (F_{i(exp)} - F_{mean})^2, \\ F &= \sum_{i=1}^{n} (F_{i(exp)} - F_{ANN})^2, \\ MSE &= \frac{1}{n} \sum_{i=1}^{n} (F_{i(exp)} - F_{i(ANN)})^2, \\ MAE &= \frac{\sum |F_{i(exp)} - F_{i(ANN)}|}{\sum F_{i(exp)}}. \end{aligned} \tag{7}$$

Table 5 represents the calculated values. As shown, the resulted errors for the testing set are quite low due to the major reduction in the training set. If we assume that the epoch value is high enough, the neural network can learn the training situation. Thus, the epoch value is a core factor in the training stage. In this study, the optimum epoch values were manually defined as almost 100. The training set error decreased by a very small value of 0.7%.

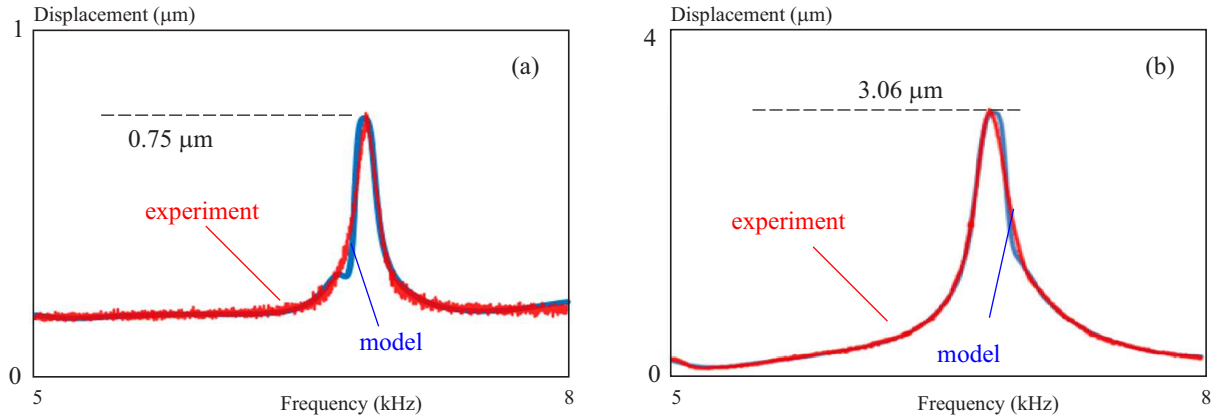

Fig. 6. Experimental and ANN modelling results for Case 6 at (a) — 0.5 V, and (b) — 5 V

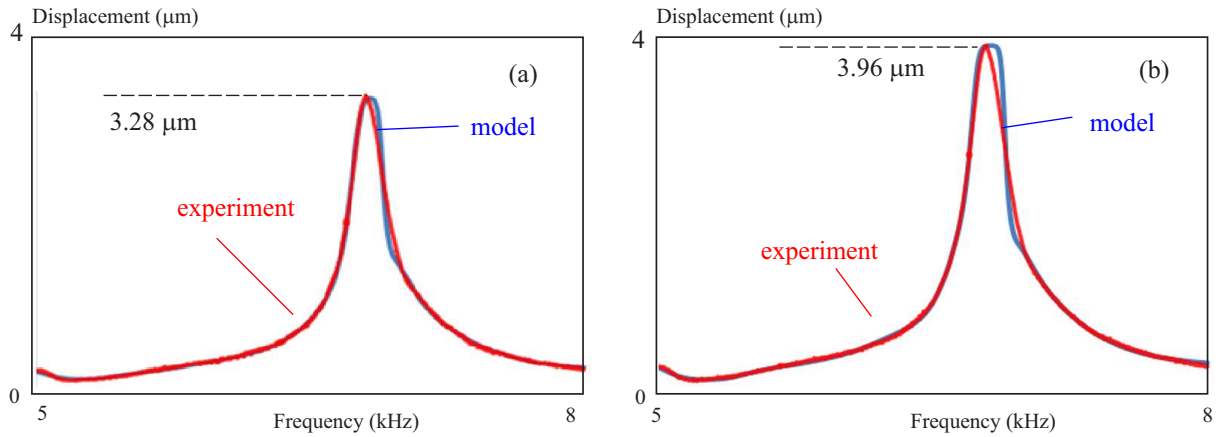

Fig. 7. Experimental and ANN modelling results for Case 6 at (a) — 5.5 V, and (b) — 10 V

Table 5. Calculated error values for six proposed configurations of training and testing sets

Case	R^2	MSE	MAE
1	0.8220	0.0005	0.3214
2	0.9986	0.0005	0.0274
3	0.9985	0.0005	0.0270
4	0.9989	0.0004	0.0239
5	0.9986	0.0005	0.0272
6	0.9936	0.0030	0.0383

Figure 4 shows the variation of MSE in ANN model according to the number of iterations. As one can see MSE value did not change significantly after the 40-th iteration (epoch).

Training R (regression) value is an indication of the relationship between the ANN modeling results and the experimental values (see Fig.5). In this study, this value was calculated as 0.99964 by ANN toolbox for Case 6. The value of $R = 1$ clearly indicates that there is an exact linear relationship between ANN modeling and the experimental values.

Figure 6 and 7 show the experimental and ANN results for Case 6 at excitation voltages from 0.5 to 10 V.

5 Evaluation of mathematical modelling and discussion

Root Mean Square Error (RMSE) is a frequently used measure of the model performance in many research studies such as metrology, mathematics and expert systems. RMSE seems to be more suitable to declare a model achievement than MAE.

In this study, we used the RMSE for the definition of the error rate of coincidence between the mathematical modelling and experimental results. The RMSE method is more preferred [28] as it can be easily implemented. If the RMSE value is close to zero, the ability of model predictions increases. Also, the acceptable error rates are varied for training process [31]. RMSE calculations are shown as a consistent value according to the equation

$$RMSE = \sqrt{\frac{1}{n}\sum_{i=1}^{n}(y_i - \hat{y}_i)^2} \tag{8}$$

where y_i is a measurement value, $\hat{y}_i$ is a predicted value, n is number of data. Table 6 shows the mean RMSE between ANN modelling and experimental results induced by the excitation voltages from 1 to 10 V.

Table 6. Consistent values in % of calculated RMSE of PEA as a result of this study

Voltage (V)	Consistency %	Error %
1	98.41	1.59
2	97.65	2.35
3	97.42	2.58
4	95.92	4.08
5	94.73	5.27
6	93.46	6.54
7	92.52	7.48
8	91.89	8.11
9	91.47	8.53
10	90.87	9.13

6 Conclusions

ANN modelling of PEA has been improved using experimental data. The dynamic displacement changes of PEA as the vibration response on the swept-sine excitation was performed. The resonant frequencies of vibrations were determined. The consistency between the obtained ANN modelling results and experimental vibration displacement values of PEA reached values from 90.3 to 98.9%, and their regression value was 0.99964. There is probably an exact linear relationship between ANN modeling and the experimental values, and the achieved ANN modelling performance demonstrates quite accurate results for all working conditions. The ANN modelling could not only avoid the complex calculation on nonlinear behaviors of PEA, but also it is more compatible to reflect the dynamical characteristics. Therefore, this ANN modelling could be recommended as training-testing tool for estimating vibration properties of PEA under any other excitation voltages.

Acknowledgements

This work was supported by the Scientific Research Council of Manisa Celal Bayar University (Project No. 2015-127).

References

[1] M. S. Vijava, *Piezoelectric Materials and Devices-Applications Engineering and Medical Sciences*, London, CRC Press Taylor&Francis Group, 2013.

[2] D. Croft, D. Shedd and S. Devasia, "Creep Hysteresis, and Vibration Compensation for Piezoactuators: Atomic Force Microscopy Application", *Journal of Dynamic Systems*, Measurement, and Control, vol. 123, no.1, pp. 35-43, November 2001.

[3] Q. Zou, K. Leang, E. Sadoun, M. Reed and S. Devasia, "Control Issues High-Speed AFM for Biological Applications: Collagen Imaging Example", *Asian Journal of Control*, vol. 6, no.2, pp. 164-178, June 2004.

[4] G. Stöppler and S. Douglas, "Adaptronic Gantry Machine Tool with Piezoelectric Actuator for Active Error Compensation of Structural Oscillations at the Tool Centre Point", *Mechatronics*, vol. 18, no.8, pp. 426-433, Oct 2008.

[5] W. Yang, S. Y. Lee and B. J. You, "A Piezoelectric Actuator with a Motion-Decoupling Amplifier for Optical Disk Drives", *Smart Material Structure*, vol. 19, no.6, 10pp. 065027, May 2010.

[6] J. J. Wei, Z. C. Qiu, J. D. Han and Y. C. Wang, "Experimental Comparison Research on Active Vibration Control for Flexible Piezoelectric Manipulator Using Fuzzy Controller", *Journal of Intelligent and Robotic System*, vol. 59, no.1, pp. 31-56, July 2010.

[7] D. E. Brehl and T. A. Dow, "Review of vibration-assisted machining", *Precision Engineering*, vol. 32, no.3, pp. 153-172, July 2008.

[8] S. R. Anton and H. A. Sodano, "A review of power harvesting using piezoelectric materials", *Smart Materials and Structures*, vol. 16, no.3, pp. R1-R21, May 2007.

[9] P. Norman, M. Backström, M. Rantatalo, A. Svoboda and A. Kaplan, "A sophisticated platform for characterization, monitoring and control of machining", *Measurement Science and Technology*, vol. 17, no.4, pp. 847-854, March 2006.

[10] X. D. Wang, N. Li, M. W. Lin and L. D. Wang, "Dynamic characteristic testing for MEMS micro-devices with base excitation", *Measurement Science and Technology*, vol. 18, no.6, pp. 1740-1747, May 2007.

[11] S. Zhen, B. Chen, L. Yuan, M. Li, J. Liang and B. Yu, "A novel interferometric vibration measurement sensor with quadrature detection based on 1/8 wave plate", *Optics and Laser Technology*, vol. 42, no.2, pp. 326-365, March 2010.

[12] S. Park, C. B. Yun, Y. Roh and J. J. Lee, "Health monitoring of steel structures using impedance of thickness modes at PZT patches", *Smart Structures and Systems*, vol. 1, no.4, pp. 339-353, Oct 2005.

[13] S. Prasad, "Two-Port Electroacoustic Model of Piezoelectric Composite Circular Plate", *Master's Thesis*, University of Florida, Gainesville, FL, USA, 2002.

[14] Q. Gallas, R. Holman, T. Nishida, B. Carroll, M. Sheplak and L. Cattafesta, "Lumped Element Modeling of Piezoelectric-Driven Synthetic Jet Actuators", *AIAA Journal*, vol. 41, no.2, pp. 240-247, February 2003.

[15] S. Prasad, Q. Gallas, S. Horowitz, B. Homeijer, B. Sankar, L. Cattafesta and M. Sheplak, "Analytical Electroacoustic Model of a Piezoelectric Composite Circular Plate", *AIAA Journal*, vol. 44, no.10, pp. 2311-2318, Oct 2006.

[16] M. Chiatto, F. Capuano, G. Coppola and L. Luca, "LEM Characterization of Synthetic Jet Actuators Driven by Piezoelectric Element: A Review", *Sensors*, vol. 17, no.6, 31pp. 1216, May 2017.

[17] L. Sui, X. Xiong and G. Shi, "Piezoelectric Actuator Design and Application on Active Vibration Control", *Physics Procedia*, vol. 25, pp. 1388-1396, 2012.

[18] C. Ru, L. Chen, B. Shao, W. Rong and L. Sun, "A hysteresis compensation method of piezoelectric actuator: Model, identification and control", *Control Engineering Practice*, vol. 17, no.9, pp. 1107-1114, September 2009.

[19] J. Peng and X. Chen, "A Survey of Modeling and Control of Piezoelectric Actuators", *Modern Mechanical Engineering*, vol. 3, pp. 1-20, February 2013.

[20] L. Parali and A. Sari, "Vibration Modelling of Piezoelectric Actuator (PEA) using Simulink Software", *ICEEE Electrical and Electronic Engineering*, 2017 4th International Conference, pp. 153-157, April 2017.

[21] W. Qingming, Z. Qiang, Z. Chi and C. Gang, "Vibration Control of Block Forming Machine Based on an Artificial Neural Network", *4th International Symposium on Neural Networks*, Nanjing, China, June 2007.

[22] X. Yang, W. Li, G. Ye and X. Su, "Hysteresis Modeling of Piezo Actuator Using Neural Networks", *IEEE International Conference on Robotics and Biomimetics (ROBIO 2008)*, Bangkok, Thailand, February 2009.

[23] K. G. Ahn, H. J. Pahk and M. Y. Jung, "A hybrid-type active vibration isolation system using neural networks", *Journal of Sound and Vibrations*, vol. 192, no.4, pp. 793-805, May 1996.

[24] "Murata Manufacturing Co. , Ltd. Piezoelectric Sound Components", [Online] http://www.murata.com/en-global/products /sound.

[25] "LK-G3000 series High-speed, High-accuracy CCD Laser Displacement Sensor", [Online] http://www.keyence.eu/products /measure/laser-1d/lk-g3000/index.jsp.

[26] L. Parali, J. Pechousek, I. Sabikoglu, P. Novak, J. Navarik and M. Vujtek, "A digital measurement system based on laser displacement sensor for piezoelectric ceramic discs vibration characterization", *Optik - International Journal for Light and Electron Optics*, vol. 127, no.1, pp. 84-89, January 2016.

[27] Y. C. Lin and C. C. Ma, "Experimental Measurement and Numerical Analysis on Resonant Characteristics of Piezoelectric Disks with Partial Electrode Designs", *IEEE Transactions on Ultrasonics*, Ferroelectrics, and Frequency Control, vol. 51, no.8, pp. 937-947, August 2004.

[28] J. Han, M. Kamber and J. Pei, *Data mining: concepts and techniques*, 3rd edition, Morgan Kaufmann Publishers, 2001.

[29] S. Wu, F. Crestani and Y. Bi, *Evaluating score normalization methods data fusion*, 3th Asia Information Retrieval Technology (AIRS'06), Beijing, China, December 2006.

[30] I. Witten and E. Frank, *Data mining: practical machine learning tools and techniques*, 2nd edition, Morgan Kaufmann series data management systems, 2005.

[31] E. L. Lehman and G. Casella, *Theory of Point Estimation*, New York, Springer, 2003.

Received 20 June 2017

Levent Paralı is an Assistant Professor in the Department of Electronics and Automation, Manisa Celal Bayar University in Turkey. His research interests include fabrications of piezoelectric actuator and sensor, and their electronic and vibration measurements.

Ali Sarı is a Lecturer in Department of Electric and Energy, Manisa Celal Bayar University in Turkey. His research interests are in the behaviors of nonlinear piezoelectric actuator analysis and theirs fault diagnosis using MATLAB.

Ulaş Kılıç is an Associate Professor in the Department of Electronics Engineering, Ege University in Turkey. His research interest contain HVDC systems, Optimal Power Flow, Transient and Voltage Stability, Heuristic Algorithms, Fuzzy Logic (ANFIS).

Özge Şahin is currently an Associate Professor at Electrical & Electronics Engineering, Dokuz Eylul University in Turkey. Her research interest include Magnetic Material Detection, Classification of Magnetic Sensors According to Various Parameters.

Jiří Pěchoušek is an Associate Professor at the Department of Experimental Physic of Faculty of Science, Palacký University in the Czech Republic. His scientific research focuses on virtual instrumentation in LabVIEW and Mössbauer spectroscopy.